Progress of Theoretical Physics, Vol. 53, No. 3, March 1975

Study of the Alpha-Clustering Structure of ^{20}Ne Based on the Resonating Group Method for $^{16}O+\alpha$

——*Analysis of Alpha-Decay Widths and the Exchange Kernel*——

Takehiro MATSUSE,[†] Masayasu KAMIMURA
and Yoshihiro FUKUSHIMA*

Department of Physics, Kyushu University, Fukuoka
**Department of Applied Physics, Fukuoka University, Fukuoka*

(Received July 15, 1974)

The alpha-clustering structure of ^{20}Ne is investigated on the basis of the one-channel resonating group method for the $^{16}O+\alpha$ system. Scattering phase shifts are calculated for $0\leq L\leq 14$ in the region $0<E_{c.m.}<45$ MeV. Energy spectra and α-decay widths of the first $K^\pi=0^\pm$ bands are well reproduced. Further discussion is made on α-spectroscopic factors, the rms distance between the c.m. of the ^{16}O and alpha cluster, intrinsic quadrupole moments and $B(E2)$ strengths for the bands. It is concluded that the $K^\pi=0^-$ band states ($L\leq 9$) have strongly an ^{16}O-α molecule-like character and that the ground band states ($L\leq 8$) have rather a shell-model-like character but can also be described fairly well within the framework of the one-channel resonating group method; the exchange kernel melts strongly the ^{16}O-α molecule-like character in the latter band. The exchange kernel is analysed by showing a kind of its equivalent local potential between the ^{16}O and alpha cluster. It is further shown that there appears an excited $K^\pi=0^+$ band with spin up to 12^+ and that the 11^- level seems to belong to the first $K^\pi=0^-$ band. Two kinds of nucleon-nucleon potentials of the reaction-matrix type and of phenomenological type are examined in the present analysis.

§ 1. Introduction

Recently much attention has been attracted to molecular aspects and alpha-like four-body correlations (alpha-correlations) in light nuclei.[1] Among the nuclei, ^{20}Ne has been extensively investigated for realizing the aspects and correlations as indispensable ones in nuclei.[2)~11)] In these investigations it has been clarified that the first $K^\pi=0^-$ rotational band built on the 5.79 MeV level has dominantly alpha-correlated properties with a molecule-like $^{16}O+\alpha$ configuration. On the other hand, it has been pointed out that the $K^\pi=0^+$ ground-state band with spin up to 8 has certain transient properties changing from the molecule-like structure to a shell-like structure (or changing in the reverse way).

It must be very important to clarify the transient properties or dual facets of the ground-state band that has been approached both by the $(sd)^4$ shell model[12] and by the various alpha-cluster models. In the study of a vertically-truncated-subspace shell model,[7] Takada and two of the present authors (M. K. and T.

[†] Present address: Research Institute for Fundamental Physics, Kyoto University, Kyoto.

M.) have shown that such dual facets can be understood fairly well within the framework of the shell model for the four valence particles but with inclusion of excited [4]-symmetry configurations higher than $(sd)^4$ ones; they have shown that certain higher-orbital-mixed configurations with the [4]-symmetry can bring about a growth of alpha-correlations. However, the spurious center-of-mass excitation in their wave function, although small, made it very difficult to estimate α-decay widths and α-spectroscopic factors which are very important quantities for investigating the alpha-correlations. Shell-model calculations of the α-decay widths of the 6^+ and 8^+ members of the ground-band states have been made by Arima and Yoshida[13] and Yazaki.[14] They give a value of only about one-fifth of the observed values using a standard oscillator parameter even if the tail of the ^{16}O-α relative wave function is improved adequately. This result seems to indicate the necessity of adding the above-mentioned higher-excited configurations to the one-major-shell ones.

In our preliminary work[9] we studied the properties of the ground-state band and the first $K^\pi=0^-$ band in calculating the α-widths on the basis of the orthogonality condition model[15] (OCM), an approximated model of the resonating group method[16] (RGM), for the $^{16}O+\alpha$ system; we solved a dynamical equation for the ^{16}O-α relative motion under the correct boundary condition for the scattering state, eliminating the forbidden states due to the Pauli principle. We have concluded that the ground-band state shows a rather shell-model-like mode in the internal region with relatively small components of the excitated states labeled as [4] $(\lambda, 0)SU_3$ higher than $(8, 0)$ one, but those higher excited components play an important role in reproducing the observed values of α-decay widths. On the other hand, we have got the following results for the $K^\pi=0^-$ band: The alpha cluster is strongly dissociated from the ^{16}O in all states whose internal wave functions have very large components (about 60% in probability) of the excited [4] $(\lambda, 0)SU_3$ states higher than $(9, 0)$ one; the $K^\pi=0^-$ band could hardly be understood within the standard shell-model picture. This result for the $K^\pi=0^-$ band is consistent with a result that was obtained by Horiuchi and Suzuki[10] in their extensive study of the α-decay widths with the use of various kinds of nuclear models.

The purpose of the present work is to perform the RGM calculation for the $^{16}O+\alpha$ system, confirm the above-mentioned understanding about the structure of ^{20}Ne and to investigate microscopically the interaction and the mechanism of particle exchange between the constituent clusters by means of analysis of the exchange kernel in RGM.

We calculate the ^{16}O-α scattering phase shifts for $0\leq L\leq 14$ and give the energy spectra, α-decay widths, α-spectroscopic factors, $B(E2)$ strengths, intrinsic quadrupole moments and the rms distance between the c.m. of ^{16}O-core and α-cluster for the first $K^\pi=0^\pm$ band states. Furthermore we show the effective potential between ^{16}O and α for investigating the role of exchange kernel and

for discussing the validity of the OCM calculation;[9] it is found that the ^{16}O-α potential shows parity-dependence but rather weak L-dependence in a space where the forbidden states due to the Pauli principle are eliminated.

As the effective two-nucleon potential, we adopt a potential of the reaction-matrix type proposed by Hasegawa, Nagata and Yamamoto[17,18] and a phenomenological one proposed by Volkov.[19] It is shown that the former potential can reproduce the observed properties of the first $K^\pi=0^\pm$ bands better than the latter one does.

We investigate also broad levels in the excited $K^\pi=0^+$ band built on the $E_x\sim 8.6$ MeV level and levels with $L\geq 10$; these levels are not reproduced by (8, 0) and (9, 0) representations of the SU_3 model.

In § 2, the RGM equations are given in a one-channel approximation. The ^{16}O-α scattering phase shifts, energy spectra and α-decay widths are obtained in § 3. In § 4, the role of an exchange kernel is discussed. Some other physical quantities are estimated in § 5 and conclusion is given in § 6.

§ 2. RGM equation and two-nucleon potential

The normalized and antisymmetrized internal wave functions of the ^{16}O and α nuclei are denoted by $\phi^{(\mathrm{in})}(^{16}\mathrm{O})$ and $\phi^{(\mathrm{in})}(\alpha)$, respectively, and are assumed to consist of the closed harmonic-cluster configuration with the common oscillator parameter $\nu=m\omega/\hbar$, m being the nucleon mass. The total wave function of ^{20}Ne is represented by

$$\Psi_{LM}(^{20}\mathrm{Ne})=\binom{20}{4}^{-1/2}\mathcal{A}\left[\phi^{(\mathrm{in})}(\alpha)\phi^{(\mathrm{in})}(^{16}\mathrm{O})u_L(R)/R\cdot Y_{LM}(\Omega_R)\right], \qquad (2\cdot1)$$

where $u_L(R)$ is the ^{16}O-α relative wave function and $\mathcal{A}$ is the antisymmetrizer intervening between the ^{16}O and α. The equation of motion for $u_L(R)$ is derived[16] from

$$\langle\phi^{(\mathrm{in})}(\alpha)\phi^{(\mathrm{in})}(^{16}\mathrm{O})\,Y_{LM}(\Omega_R)\,|H-E_{\mathrm{total}}|\Psi_{LM}(^{20}\mathrm{Ne})\rangle_R=0\,, \qquad (2\cdot2)^{*)}$$

where E_{total} is the total energy and H is the total Hamiltonian

$$H=-\sum_{i=1}^{20}\frac{\hbar^2}{2m}\nabla^2-T_G+\sum_{i<j}^{20}(v_{ij}^{(N)}+v_{ij}^{(C)}). \qquad (2\cdot3)$$

Here $v_{ij}^{(N)}$ and $v_{ij}^{(C)}$ denote the two-nucleon central potential and Coulomb potential, respectively, and T_G the kinetic-energy operator of the center-of-mass coordinate.

From Eq. (2·2), we obtain the integro-differential equation

$$\left[-\frac{\hbar^2}{2\mu}\cdot\frac{d^2}{dR^2}+\frac{\hbar^2L(L+1)}{2\mu R^2}+V_D^{(N)}(R)+V_D^{(C)}(R)-(E_{\mathrm{total}}-E_{\mathrm{in}})\right]u_L(R)$$
$$=-\int_0^\infty\left[G_L(R,R')+E_{\mathrm{total}}K_L(R,R')\right]u_L(R')\,dR', \qquad (2\cdot4)$$

*) The bracket $\langle|\rangle_R$ denotes the quantity integrated over all the variables except for R, while hereafter $\langle|\rangle$ indicates the quantity integrated over all the variables involved.

where $V_D^{(N)}$ and $V_D^{(C)}$ denote the direct nuclear and Coulomb potentials, respectively, E_{in} the sum of calculated internal energies of the ^{16}O and α nuclei and μ the reduced mass; K_L is the exchange overlap kernel and G_L the exchange kernel of the kinetic energy and the two-body nuclear and Coulomb potentials. The energy of relative motion, E, measured on the center-of-mass system is given by

$$E=E_{\text{total}}-E_{\text{in}}\,. \tag{2·5}$$

Here the two-nucleon potential $v_{ij}^{(N)}$ is approximated by the superposed form with several-range Gaussians:

$$v_{ij}^{(N)}=\sum_n [{}^{13}V_n\,{}^{13}P(ij)+{}^{31}V_n\,{}^{31}P(ij)+{}^{33}V_n\,{}^{33}P(ij)+{}^{11}V_n\,{}^{11}P(ij)]\exp(-r_{ij}^2/r_{0n}^2), \tag{2·6}$$

where ${}^{2T+1,2S+1}P(ij)$ is the projection operator to the state of isospin T and spin S. The explicit forms of $V_D^{(N)}$, $V_D^{(C)}$ and E_{in} have been given in our previous paper.[20]

We expand the kernels K_L and G_L in the forms

$$K_L(R,R')=\sum_N k_N^{(L)}u_{NL}(R)\,u_{NL}(R'),$$
$$G_L(R,R')=\sum_{N,N'} g_{NN'}^{(L)}u_{NL}(R)\,u_{N'L}(R'), \tag{2·7}$$

where $u_{NL}(R)$ is the harmonic oscillator function with oscillator parameter $(16/5)\nu$. An analytical method for deriving these coefficients has been shown in our previous work,[20] and another method has been proposed by Suzuki.[21] The expansions with $2N+L\leq 30$ give a very sufficient approximation in the present calculation.

We use the following two types of effective potentials as $v_{ij}^{(N)}$, their parameters are listed in Table I.

(I) A potential of the reaction-matrix type given by Hasegawa, Nagata and Yamamoto;[17),18] it is referred to as HNY potential. This three-range Gaussian potential is made by modifying slightly the potential that has been

Table I. Parameters of the two-nucleon central potential Eq. (2·6), in which $n=1$, 2 and 3 correspond to the OPEP, medium-range force and short-range force, respectively. HNY (Hasegawa-Nagata-Yamamoto) potential is of the reaction-matrix type. For Volkov potential (no $n=1$) the No. 2 type with $m=0.62$ is chosen.

name	n	range r_{0n}(fm)	depth (MeV)			
			${}^{13}V$	${}^{31}V$	${}^{33}V$	${}^{11}V$
HNY potential	1	2.5	−6.0	−5.0	5/3	15.0
	2	0.942	−524.7	−360.0	−50.0	50.0
	3	0.542	1655.0	1145.0	162.0	0.0
Volkov potential	2	1.80	−60.65	−60.65	14.56	14.56
	3	1.01	61.14	61.14	−14.67	−14.67

proposed by Hasegawa and Nagata[17] in their study of ^{6}Li; only the depth ^{13}V of the medium-range part is changed[18b] from -546.0 MeV to -524.7 MeV by approximating a starting-energy-dependent interaction in the reaction-matrix method for the ^{16}O-α system.[18a] Hasegawa and Nagata have constructed the even-state parts of their potential by strengthening slightly the reaction-matrices calculated from OPEG (a Gauss soft-core potential with the one-pion-exchange tail)[22] so as to reproduce the binding energy and rms radius of ^{4}He. They have chosen odd-state potentials to approximate the long- and medium-range parts of the OPEG, referring to the result of α-α scattering by the RGM calculation;[23] the matrix elements of these odd-state potentials are similar to the reaction matrices solved on the alpha-cluster intrinsic basis in ^{8}Be nucleus.[24]

(II) A phenomenological effective potential given by Volkov[19] as the type No. 2. Here the Majorana-mixture parameter $m=0.62$ is chosen. This potential is referred to as Volkov potential.

§ 3. Energy spectra and reduced α-widths

Equation (2·4) is solved subject to the usual boundary condition for the bound state or scattering state.*) The energy of resonance state $E^{(\mathrm{res})}$ is decided from the condition

$$\delta_L(E)|_{E=E^{(\mathrm{res})}}=\frac{\pi}{2}\pm n\pi \quad \text{and} \quad \frac{d}{dE}\delta_L(E)|_{E=E^{(\mathrm{res})}}>0\,, \tag{3·1}$$

where δ_L is the scattering phase shift, n being an arbitrary integer.

The α-width of the resonance state is estimated by

$$\Gamma_\alpha^{\mathrm{cal}}=-4/\frac{d}{dE}(\mathrm{Im}\,\eta_L)|_{E=E^{(\mathrm{res})}}, \tag{3·2}$$

where η_L is the scattering amplitude. We introduce the reduced α-width γ_α^2 by

$$\Gamma_\alpha=2ka\gamma_\alpha^2(a)/[F_L^2(ka)+G_L^2(ka)]. \tag{3·3}$$

Here F_L and G_L are the regular and irregular Coulomb functions, respectively, and a is the channel radius; k is the wave number of calculated (observed) resonance state, $k^2=2\mu E^{(\mathrm{res})}/\hbar^2$. Furthermore we define a non-dimensional reduced α-width θ_α^2 as the ratio of the reduced α-width γ_α^2 to its Wigner limit $\gamma_W^2(a)=3\hbar^2/(2\mu a^2)$:

$$\theta_\alpha^2(a)=\gamma_\alpha^2(a)/\gamma_W^2(a). \tag{3·4}$$

Hereafter we simply call θ_α^2 the reduced α-width and discuss it.

*) For the scattering state, Eq. (2·4) is solved by an application[25] of Kohn's variational principle.[26] The harmonic oscillator functions $u_{NL}(R)$ with $\max\{0,\ 4-[L/2]\}\leq N\leq 12-[L/2]$ are used as the variational functions in the internal region. This method gives high numerical accuracy and sufficiently short computing-time in the present calculation.

In order to see the behaviour of ^{16}O-α relative motion, we define the reduced width amplitude[27] $y_L(R)$ as

$$y_L(R) = \binom{20}{4}^{1/2} R\langle \phi^{(\mathrm{in})}(\alpha)\phi^{(\mathrm{in})}(^{16}\mathrm{O})\, Y_{LM}(\Omega_R) \,|\, \Psi_{LM}(^{20}\mathrm{Ne})\rangle_R$$
$$= \int_0^\infty [\delta(R,R') - K_L(R,R')]u_L(R')dR', \qquad (3\cdot5)$$

where the resonance-state wave function $\Psi_{LM}(^{20}\mathrm{Ne})$ is normalized within the internal region $R<10$ fm.

In the present calculation, the oscillator parameter of the ^{16}O and α-cluster is chosen as $\nu = m\omega/\hbar = 0.32\ \mathrm{fm}^{-2}$.

Table II gives the observed value of energy E and reduced α-widths θ_α^2 of the levels that are discussed in this work. Since the reduced α-width represents a degree of alpha-cluster dissociation, we can see a clear difference in the degree between the first $K^\pi=0^\pm$ bands; the alpha cluster has a much larger probability of being found in the $K^\pi=0^-$ band with $L\leq 9$ than in the ground-state band with $L\leq 8$ (the α-widths in the $K^\pi=0^-$ band become about Wigner limit at $a\approx 5$ fm).

Calculated energies E and reduced α-widths θ_α^2 of the first $K^\pi=0^\pm$ band levels ($L\leq 9$) and of the 10^+ and 11^- levels are shown in Table III and Fig. 1. It is remarkable that the observed level structures, reduced α-widths of the two bands and the ^{16}O-α threshold energy ($E_x=4.73$ MeV) are simultaneously

Table II. Observed energies E, α-decay widths Γ_α and reduced α-decay widths θ_α^2(a) of the levels in the first $K^\pi=0^\pm$ bands and an excited $K^\pi=0^+$ band of ^{20}Ne.

L^π	E (E_x) (MeV)	Γ_α (KeV)	θ_α^2(a)	
			$a=5$ fm	$a=6$ fm
0^+	−4.73 (0.0)	—	—	—
2^+	−3.10 (1.63)	—	—	—
4^+	−0.48 (4.25)	—	—	—
6^+	4.05 (8.78)	0.110±0.025	0.075 ±0.017	0.0105 ±0.0024
8^+	7.22 (11.95)	0.035±0.010	0.0098±0.0028	0.00097±0.00028
1^-	1.06 (5.79)	>0.013	>0.46	>0.14
3^-	2.44 (7.17)	8	0.91	0.26
5^-	5.53 (10.26)	141	1.06	0.31
7^-	10.7 (15.4)	380	0.82	0.25
9^-	18.0 (22.7)	500	0.53	0.17
0^+	~3.9 (~8.6)	>800	>0.49	>0.42
2^+	~4.1 (~8.8)	>800	>0.93	>0.61
4^+	6.06 (10.79)	349	0.43	0.23

Experimental values are taken from Ref. 38) There are some other 9^- levels: i) $E_x=20.68$ MeV, $\Gamma_\alpha=120$ KeV, $\theta_\alpha^2(5\mathrm{fm})=0.27$, ii) $E_x=21.08$ MeV, $\Gamma_\alpha=80$ KeV, $\theta_\alpha^2(5\mathrm{fm})=0.15$ and iii) $E_x=22.84$ MeV, $\Gamma_\alpha=250$ KeV, $\theta_\alpha^2(5\mathrm{fm})=0.25$.

Table III. Calculated energies E and reduced α-widths $\theta_\alpha^2(a)$ of the first $K^\pi=0^\pm$ band levels ($L\leq 9$) and of the 10^+ and 11^- levels in ^{20}Ne. Energies E are measured with respect to the calculated ^{16}O-α threshold energy.

(a) HNY-potential case

L^π	E (MeV)	$\theta_\alpha^2(a)$ a=5 fm	$\theta_\alpha^2(a)$ a=6 fm
0^+	−4.86	—	—
2^+	−3.83	—	—
4^+	−1.50	—	—
6^+	1.97	0.13	0.014
8^+	6.24	0.027	0.0024
10^+	25.8	1.36	0.65
1^-	1.13	1.08	0.34
3^-	2.90	1.02	0.34
5^-	6.19	1.03	0.36
7^-	11.22	0.96	0.33
9^-	18.10	0.59	0.20
11^-	34.3	1.87	1.11

(b) Volkov-potential case

L^π	E (MeV)	$\theta_\alpha^2(a)$ a=5 fm	$\theta_\alpha^2(a)$ a=6 fm
0^+	−4.26	—	—
2^+	−3.25	—	—
4^+	−0.94	—	—
6^+	2.52	0.49	0.054
8^+	6.77	0.16	0.015
10^+	23.2	2.68	0.99
1^-	0.30	2.20	0.57
3^-	1.98	2.23	0.58
5^-	5.08	2.28	0.60
7^-	9.89	2.28	0.61
9^-	16.74	1.62	0.44
11^-	31.1	2.96	1.43

The calculated value of the total energy E_{total} of the ground state is −119.1 MeV for HNY potential and −140.0 MeV for Volkov potential, while its observed value is −160.6 MeV.

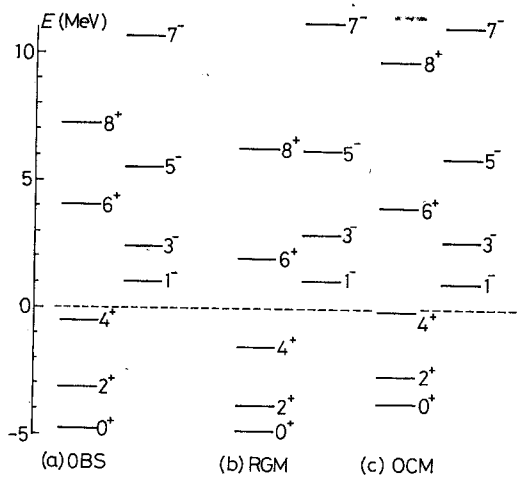

Fig. 1. Energy spectra of the first $K^\pi=0^\pm$ bands in ^{20}Ne; (a) observation, (b) result of the RGM calculation and (c) result of the OCM calculation with Eq. (4·5).

reproduced fairly well by using the HNY potential; a similar result is given by using Volkov potential with $m=0.62$ except for reduced α-widths. Volkov potential seems to cause rather too strong dissociation of the alpha cluster, especially in the ground-band state.*)

Figure 2 illustrates the reduced

*) If we try to use $\nu=0.40$ fm^{-2} as the oscillator parameter instead of $\nu=0.32$ fm^{-2} in the case of Volkov potential with $m=0.62$, the reduced α-widths are rather improved in some states, but they are still fairly too large in the 6^+, 8^+, 7^- and 9^- states. Furthermore the rms radius of the ground state shrinks to 2.69 fm from 2.94 fm of the case $\nu=0.32$ fm^{-2} (cf. § 5); the former radius is much too small compared with its observed value 2.90~2.96 fm.[28] Taking these results into account, we then use $\nu=0.32$ fm^{-2} both for Volkov potential and for HNY potential in the present work.

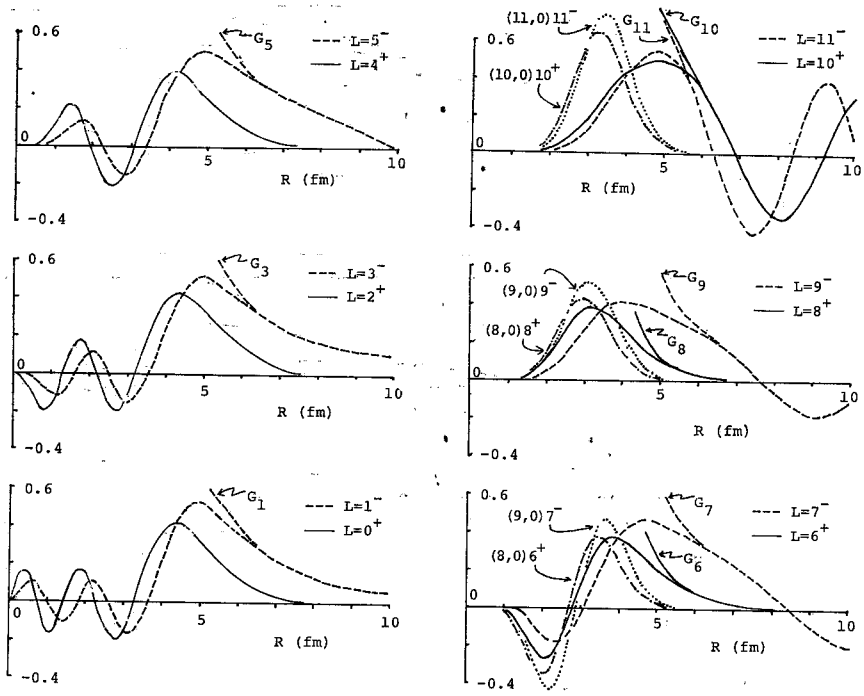

Fig. 2. Reduced width amplitudes $y_L(R)$ of the levels in the first $K^\pi=0^\pm$ bands ($L\leq 9$) and of the 10^+ and 11^- levels. Furthermore, $y_L(R)$ of several $(\lambda, 0)SU_3$ states are given and the irregular Coulomb function $G_L(kR)$ are illustrated, being normalized to $y_L(R)$ at the asymptotic region. $y_L(R)$ are given in units of $\mathrm{fm}^{-1/2}$.

width amplitude $y_L(R)$ in the HNY-potential case. We can see again that the alpha cluster shows a much stronger dissociation in the $K^\pi=0^-$ band state than in the ground-band state; however, even for the latter band state the growth of alpha-correlations is clearly seen in comparing $y_L(R)$ of the state with that of the $(8, 0)SU_3$ state.

A decrease of the reduced α-width with increasing spin is observed in the higher spin members of both the $K^\pi=0^\pm$ bands (Table II) and is well reproduced in the calculation (Table III); this seems to indicate a shrinking of the rms distance between the c.m. of ^{16}O and α-cluster in ^{20}Ne with spin-increasing[5),13),29)] (cf. § 5).

Referring to the calculated result for the $K^\pi=0^-$ band, we predict the α-width Γ_α of the 1^- level ($E_x=5.79$ MeV) to be about 35 eV and consider the 9^- level observed at $E_x=22.7$ MeV with $\Gamma_\alpha=500$ KeV to be the member of the first $K^\pi=0^-$ band, those conjectures are consistent with those given by Arima and Yoshida.[13b)]

Figure 3 shows the ^{16}O-α scattering phase shifts $\delta_L(E)$ for $0\leq L\leq 14$ in the HNY-potential case (a very similar pattern is obtaind in the Volkov-potential

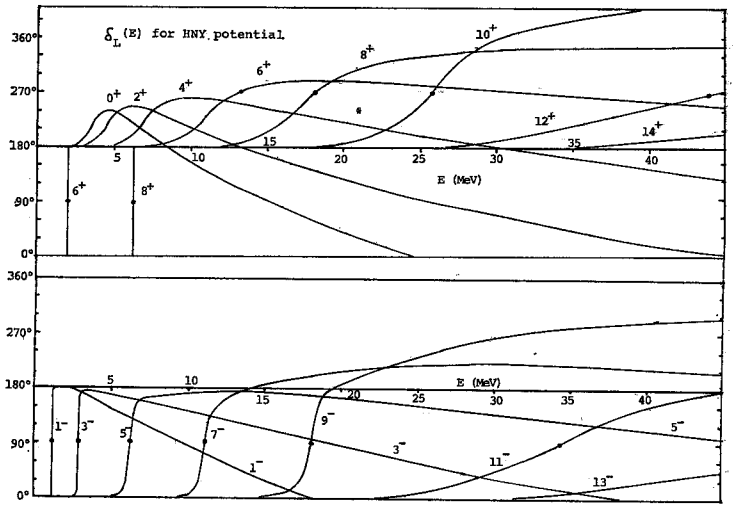

Fig. 3. Calculated ^{16}O-α scattering phase shifts δ_L vs. the c.m. scattering energy E in the HNY-potential case. There appear very broad resonances at 54.0 MeV (13^-) and 66.4 MeV (14^+).

case). The ground-state band is surely composed of levels with spin up to 8. We can recognize existence of an excited $K^\pi=0^+$ band*) which consists of broad resonance levels with spin up to 12, although we have not 0^+, 2^+ and 4^+ resonances in the strict sense of the condition (3·1); this band is considered to correspond to the observed $K^\pi=0^+$ band starting from the 0^+ level at $E_x\sim 8.6$ MeV (cf. Table II). We consider that the 12^+ resonance state can be regarded as a member of the excited $K^\pi=0^+$ band, and therefore that this band is not the $(10,0)SU_3$ band, but is mainly composed of the $(12,0)SU_3$ and more-excited $(\lambda,0)$ configurations.**) Indeed, the $y_L(R)$ of the 10^+ level, for example, deviates much from that of the $(10,0)$ state in the internal region (Fig. 2).

In Fig. 3 no excited $K^\pi=0^-$ band can be considered to appear. The first $K^\pi=0^-$ band seems to reach the 11^- level; the difference in the reduced α-width between the 11^- and 9_1^- levels is not so large as the difference between the 10^+ level of the excited $K^\pi=0^+$ band and the 8_1^+ level of the first $K^\pi=0^+$ band. This continuity from the 9_1^- to 11^- level, although rather weak, indicates that the levels with $L\leq 9$ in the first $K^\pi=0^-$ band have large components of the $(11,0)SU_3$ and more excited configurations[5] (cf. Table V).

*) Existence of the resonance or resonance-like levels with the lower spins in this band is predicted in Refs. 6), 8) and 32) on the basis of microscopic calculation for ^{16}O-α scattering.

**) This band has been considered to be composed of a $(pf)^4$ "quartet" in Ref. 35). The result of two-nucleon transfer experiment ^{18}O(^{11}B, ^{9}Li)^{20}Ne shows[36] that it is $(pf)^4$ rather than $(sd)^2(pf)^2$ band.

§ 4. The role of exchange kernel

For the sake of simplicity in expression, we put

$$\mathcal{L}_L(R) \equiv -\frac{\hbar^2}{2\mu}\cdot\frac{d^2}{dR^2}+\frac{\hbar^2 L(L+1)}{2\mu R^2}+V_D^{(N)}(R)+V_D^{(C)}(R)-E\,,$$

$$\mathcal{W}_L(R,R') \equiv G_L(R,R')+E_{\text{total}}K_L(R,R') \tag{4·1}$$

and write Eq. (2·4) in the form

$$\mathcal{L}_L u_L = -\mathcal{W}_L u_L\,. \tag{4·2}$$

We introduce the following projection operator Λ_L:

$$\Lambda_L(R,R') = \delta_L(R,R') - \sum_{N=0}^{2N+L<8} u_{NL}(R)\,u_{NL}(R')\,, \tag{4·3}$$

which eliminates the redundant solutions $\{u_{NL}(R);\ 2N+L<8\}$ of Eq. (4·2). By the use of Λ_L, Eq. (4·2) is rewritten as[15]

$$\Lambda_L\mathcal{L}_L\Lambda_L u_L = -\Lambda_L\mathcal{W}_L\Lambda_L u_L\,. \tag{4·4}$$

In order to investigate the role of the exchange kernel $\Lambda_L\mathcal{W}_L\Lambda_L$, we first drop it in Eq. (4·4) and solve the following equation of the orthogonality condition model[15] (OCM):

$$\Lambda_L\mathcal{L}_L\Lambda_L u_L = 0\,. \tag{4·5}$$

Calculated energy spectra are shown in Fig. 1 in the HNY-potential case. It is surprising that although $\Lambda_L\mathcal{W}_L\Lambda_L$ is dropped, the level structure of the $K^\pi = 0^-$ band changes little and that of the ground-state band does not show so drastic change (a very similar result is obtained in the Volkov-potential case); this fact asserts to a certain extent the validity of the OCM calculation for the low-lying levels of the $^{16}O+\alpha$ system.[9),*)] On the other hand, the reduced α-widths calculated with the approximated equation (4·5) become much larger (about several times as large as that in the $K^\pi=0^+$ band and about 1.7 times as large as that in the $K^\pi=0^-$ band) than those calculated with the RGM equation (4·4); this indicates that the exchange kernel $\Lambda_L\mathcal{W}_L\Lambda_L$ affects strongly the surface behaviour of the ^{16}O-α relative motion.

In order to visualize the function of the exchange kernel, we introduce a kind of local potential $V_{\text{exch}}^{(L)}(R)$ for a given wave function $u_L(R)$ in the form

$$\Lambda_L V_{\text{exch}}^{(L)}\Lambda_L u_L = \Lambda_L\mathcal{W}_L\Lambda_L u_L\,. \tag{4·6}$$

*) If we use the two-nucleon potential given by Brink and Boeker[30] as type No. 1 which has very strong exchange character, $V_D^{(N)}(R)$ is strongly repulsive (about 300 MeV at $R=0$) and the exchange kernel shows stronger attractive effect (about -400 MeV at $R\approx 0$ for the $V_{\text{exch}}^{(L)}(R)$ defined in Eq. (4·6)). In this case the OCM does not work. The observed energy spectra and reduced α-widths are not reproduced so well in the RGM calculation by using this two-nucleon potential.

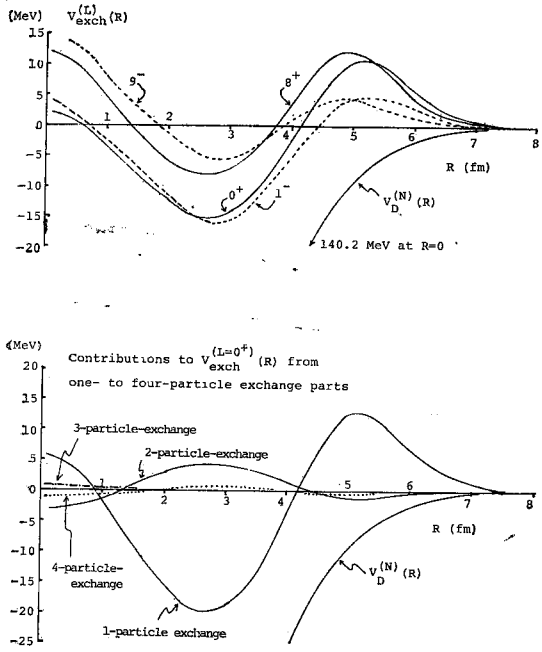

Fig. 4. The effective-local ^{16}O-α potential $V^{(L)}_{exch}(R)$ coming from the whole exchange kernel, and contributions to the $V^{(L)}_{exch}(R)$ of the ground state from the one- to four-particle exchange parts in $\mathcal{W}_L$ (the HNY-potential case).

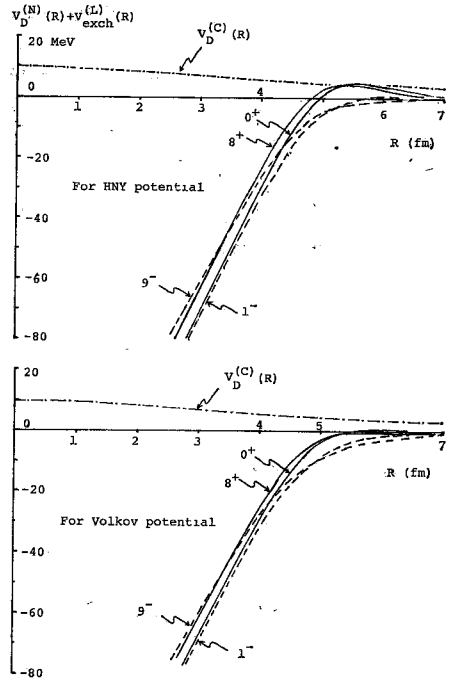

Fig. 5. Surface-behaviour of the effective-local ^{16}O-α potential $V^{(N)}_D(R)+V^{(L)}_{exch}(R)$ for the first $K^\pi=0^\pm$ band states.

The $V^{(L)}_{exch}(R)$ is given[25b] uniquely without any divergence in the vicinity of the radial nodes in the inner oscillation of $\Lambda_L u_L$. In Fig. 4, $V^{(L)}_{exch}(R)$ for the first $K^\pi=0^\pm$ band states are shown in the HNY-potential case. Also in Fig. 4, we show contributions to the $V^{(L)}_{exch}(R)$ from the one- to four-particle exchange parts[20] of $\mathcal{W}_L$ in the case of the ground state; the one-particle exchange part is dominant and this is seen in other low-lying states.*) The $V^{(L)}_{exch}(R)$ is found to reduce the relative-motion amplitude in the surface region and enhance it in the inner region; this role of $\mathcal{W}_L$ decreases the reduced α-width of the RGM calculation from the value of the OCM one.

Next, we consider the equation

$$\Lambda_L(\mathcal{L}_L+V^{(L)}_{exch})\Lambda_L u_L=0 \qquad (4\cdot7)$$

to be a kind of the OCM equation in which the effect of the exchange kernel is included in a state-dependent way. In Fig. 5, we show the surface-region behaviour of the total effective-local potential $V^{(N)}_D(R)+V^{(L)}_{exch}(R)$; the potential should be regarded as a kind of local potential only in the space where the

*) A similar analysis has been reported in Ref. 31).

redundant solutions $u_{NL}(R)$ with $2N+L<8$ are forbidden. This type of effective ^{16}O-α potential shows very little shrinkage of its effective radius with increasing spin in each of the $K^\pi=0_1^\pm$ bands ($L\leq 9$);*) this feature presents a contrast to the clear shrinkage of the mass-distribution radius with increasing spin (cf. § 5). This result offers a microscopic basis to the phenomenological OCM analysis[9] in which the radius of the effective ^{16}O-α potential of Woods-Saxon type is fixed in each of the $K^\pi=0_1^\pm$ bands in contrast with the treatment shown by Arima and Yoshida[18] in their extensive study of α-widths. From Fig. 5, however, we can say that the diffuseness parameter rather than the radius parameter was to be changed effectively between the $K^\pi=0_1^+$ and $K^\pi=0_1^-$ bands in that OCM analysis.

It is very interesting to see in Fig. 5 that for the ground-band state in the HNY-potential case the effective ^{16}O-α potential $V_D^{(N)}(R)+V_{\rm exch}^{(L)}(R)$ is repulsive in the outer part of the surface region; that is, there the effect of the particle-exchange kernel $\mathcal{W}_L$ is repulsive and stronger than the attractive ^{16}O-α direct potential $V_D^{(N)}(R)$. This role**) of the ^{16}O-α potential $V_D^{(N)}(R)+V_{\rm exch}^{(L)}(R)$ pulls strongly the alpha cluster inside the surface region, giving a large overlapping between the ^{16}O and α (cf. the rms distance between the two clusters given in Table V), and therefore the Pauli principle works strongly so as to dissolute the clusters into a rather shell-model-like wave function in the ground-band state.

§ 5. α-spectroscopic factor, rms distance between ^{16}O and α, intrinsic quadrupole moment and $B(E2)$ strength

As far as the resonance state is concerned, it seems to us very difficult to calculate physical quantities such as the α-spectroscopic factor, rms distance between ^{16}O and α, intrinsic quadrupole moment and $B(E2)$ value, with correct treatment of the integration over the relative coordinate R. Therefore, throughout this section we adopt a bound-state approximation for the resonance state in estimating such quantities.

First we introduce ortho-normalized basic functions $\Psi_{NLM}(^{20}\mathrm{Ne})$ with $2N+L\geq 8$ as

$$\Psi_{NLM}(^{20}\mathrm{Ne})=S_{NL}^{-1}\binom{20}{4}^{-1/2}\mathcal{A}\left[\phi^{(\mathrm{in})}(\alpha)\phi^{(\mathrm{in})}(^{16}\mathrm{O})u_{NL}(R)/R\cdot Y_{LM}(\Omega_R)\right], \quad (5\cdot 1)$$

where $S_{NL}=(1-k_N^{(L)})^{1/2}$. The $\Psi_{NLM}(^{20}\mathrm{Ne})$ is related[34] to the SU_3 wave function $\Phi_{LM}((\lambda,0))$ with $\lambda=2N+L$ that has the label $[4](\lambda,0)$ and the $(\lambda-8)\hbar\omega$ in-

*) In the $V_D^{(N)}(R)+V_{\rm exch}^{(L)}(R)$ of Fig. 5, the radius giving a half of the maximum depth is about 3.1 fm for the $K=0_1^+$ band and about 3.3 fm for the $K=0_1^-$ band in both the HNY- and Volkov-potential cases; the deviation from the value in each band is less than 0.1 fm.

**) In this role the lack of the long-range part of $V_D(R)$ in the HNY-potential case is of importance; this comes from the property of the outermost part (corresponding to OPEP) of this nucleon-nucleon potential (Hiura and Tamagaki, Chapter II of Ref. 1)). Such an effect does not appear in the phenomenological Volkov potential.

trinsic excitation with respect to the (8, 0) state:

$$\Phi_{LM}((\lambda,0)) = (20\nu/\pi)^{3/4} e^{-10\nu R_G^2} \Psi_{NLM}(^{20}\mathrm{Ne}). \quad (\lambda = 2N+L) \tag{5·2}$$

Next we diagonalize the Hamiltonian (2·3) within the subspace $\{\Psi_{NLM}(^{20}\mathrm{Ne}); N_{\min} \leq N \leq N_{\max}\}$;*) here $N_{\min} = 4 - [L/2]$ for $L \leq 9$ and $N_{\min} = 0$ for $L \geq 10$. In other words we solve Eq. (2·4) assuming the following expansion of $u_L(R)$:

$$u_L(R) = \sum_{N=N\min}^{N\max} (C_{NL}/S_{NL})\, u_{NL}(R). \tag{5·3}$$

The normalization condition is expressed as

$$\langle \Psi_{LM}(^{20}\mathrm{Ne}) | \Psi_{LM}(^{20}\mathrm{Ne}) \rangle = \sum_{N=N\min}^{N\max} C_{NL}^2 = 1. \tag{5·4}$$

By the use of the coefficients C_{NL} the total wave function is expanded in terms of the $(2N+L, 0)SU_3$ states:

$$(20\nu/\pi)^{3/4} e^{-10\nu R_G^2} \Psi_{LM}(^{20}\mathrm{Ne}) = \sum_{N=N\min}^{N\max} C_{NL} \Phi_{LM}((2N+L, 0)). \tag{5·5}$$

The reduced width amplitude (3·5) is approximated by

$$y_L(R) = \sum_{N=N\min}^{N\max} C_{NL} S_{NL} u_{NL}(R). \tag{5·6}$$

Figure 6 illustrates the effect of space-truncation on the energy spectra

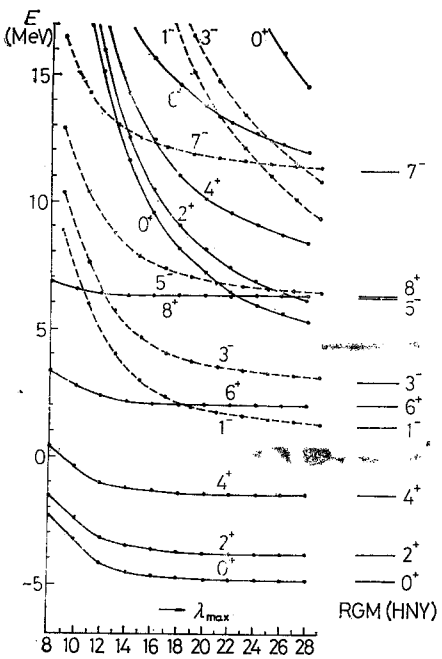

Fig. 6. Dependence of the energy spectra of ^{20}Ne on the space truncation. The total Hamiltonian is diagonalized within the $(\lambda, 0)SU_3$ subspace, $\{\Phi_{LM}((\lambda, 0)); 2N_{\min} + L \leq \lambda \leq \lambda_{\max}\}$. The abscissa denotes the value of $\lambda_{\max} = 2N_{\max} + L$. The energy spectra obtained before under the correct boundary condition are shown on the right of the curves. It should be noted that some levels appearing in the bound-state approximation are not at all resonance-like under the correct boundary condition (cf. Fig. 3).

*) Work based on this procedure is also given in Refs. 31) and 33). In the latter work[33] the case in which the configurations with $(sd)^4[31]$ and $(sd)^4[4](4, 2)$, $(0, 4)$ and $(2, 0)$ are further included, is also investigated.

($N_{\max}$-dependence).

The resonance energies that are obtained in § 3 under the correct boundary condition are reproduced well with the truncation $2N_{\max}+L=28(=29)$ for the first $K^\pi=0^+(=0^-)$ band states with spin $L\leq 8(L\leq 9)$; as far as these states are concerned, deviation of the approximated $y_L(R)$ from the exact solution (3·5) is found to be small in the region $R\leq 6$ fm. Throughout § 5 this truncation is adopted.

The expansion coefficients C_{NL} in (5·5) are shown in Table IV. The $(8, 0)SU_3$ state is of course dominant in the ground-band state, but the mixing of the higher $(\lambda, 0)SU_3$ states gives rise to a large enhancement of the surface-region amplitude of the ^{16}O-α relative motion (cf. the cases $L=6$ and 8 in Fig. 2). On the other hand, in the first $K^\pi=0^-$ band the strong distribution of the amplitudes C_{NL} into higher $(\lambda, 0)$ states is clearly seen; this can be regarded as an SU_3-model representation of the ^{16}O-α molecule-like structure. The increase of the lowest $(\lambda, 0)$ component with increasing spin in each of the first $K^\pi=0^\pm$ bands ($L\leq 9$) indicates that the alpha-correlations (alpha-dissociation) become weak as spin increases in the band.

Table IV. Expansion coefficients C_{NL} of the total wave function in terms of the $(2N+L, 0)$ SU_3 states. Use is made of the bound-state approximation for resonance state (cf. Eq. (5·5)). First several C_{NL} are given for each level in the HNY-potential case. E_{bound} gives the energy obtained by the bound-state approximation, while E gives the energy obtained before under the correct boundary condition.

L^π	E_{bound} (E) (MeV)	C_{NL} of $(2N+L, 0)$ SU_3 state					
		(8, 0)	(10, 0)	(12, 0)	(14, 0)	(16, 0)	(18, 0)
0^+	−4.86 (−4.86)	0.897	−0.323	0.237	−0.139	0.094	−0.062
2^+	−3.83 (−3.83)	0.903	−0.315	0.229	−0.133	0.090	−0.059
4^+	−1.50 (−1.50)	0.920	−0.293	0.209	−0.119	0.080	−0.052
6^+	1.97 (1.97)	0.946	−0.250	0.169	−0.092	0.060	−0.039
8^+	6.24 (6.24)	0.976	−0.177	0.106	−0.053	0.033	−0.021
0^+	5.22 —[a]	−0.375	−0.344	0.375	−0.411	0.380	−0.337
2^+	6.15 —[a]	−0.363	−0.352	0.378	−0.411	0.380	−0.336
4^+	8.34 —[a]	−0.332	−0.370	0.387	−0.411	0.378	−0.336
10^+	24.4 (25.8)	—	−0.451	0.378	−0.371	0.363	−0.349
		(9, 0)	(11, 0)	(13, 0)	(15, 0)	(17, 0)	(19, 0)
1^-	1.28 (1.13)	0.670	−0.458	0.377	−0.289	0.226	−0.174
3^-	3.09 (2.90)	0.675	−0.456	0.372	−0.286	0.224	−0.174
5^-	6.41 (6.19)	0.689	−0.449	0.361	−0.279	0.221	−0.174
7^-	11.34 (11.22)	0.718	−0.433	0.339	−0.263	0.212	−0.171
9^-	18.05 (18.10)	0.787	−0.386	0.285	−0.225	0.187	−0.158
11^-	28.8 (34.3)	—	−0.218	0.218	−0.340	0.384	−0.407

a) There is no corresponding resonance in the strict sense of (3.1), but see the phase shift behaviour in Fig. 3.

The α-spectroscopic factor S_α^2 of the $0s$ four-nucleon cluster in ^{20}Ne is defined as

$$S_\alpha^2 = \int_0^\infty y_L^2(R)\,dR = \sum_{N=N\min}^{N\max} C_{NL}^2 S_{NL}^2 . \qquad (5\cdot7)$$

The mean square radius of the state $\Psi_{LM}(^{20}\mathrm{Ne})$ measured with respect to the c.m. of ^{20}Ne, $\boldsymbol{R}_G$, is calculated by

$$\langle r^2\rangle_{^{20}\mathrm{Ne}} = \langle \Psi_{LM}(^{20}\mathrm{Ne}) | \frac{1}{20}\sum_{i=1}^{20} (\boldsymbol{r}_i - \boldsymbol{R}_G)^2 | \Psi_{LM}(^{20}\mathrm{Ne})\rangle . \qquad (5\cdot8)$$

Let $\langle r^2\rangle_{^{16}\mathrm{O}}$ and $\langle r^2\rangle_\alpha$ denote the mean square radii for $\phi^{(\mathrm{in})}(^{16}\mathrm{O})$ and $\phi^{(\mathrm{in})}(\alpha)$, respectively, and $\langle R^2\rangle$ the mean square distance between the c.m. of ^{16}O and α in the state $\Psi_{LM}(^{20}\mathrm{Ne})$. The $\langle R^2\rangle$ can then be estimated from the equation

$$20\langle r^2\rangle_{^{20}\mathrm{Ne}} = 16\langle r^2\rangle_{^{16}\mathrm{O}} + 4\langle r^2\rangle_\alpha + \frac{16}{5}\langle R^2\rangle , \qquad (5\cdot9)$$

where $\langle r^2\rangle_{^{16}\mathrm{O}} = 69/32\nu$ and $\langle r^2\rangle_\alpha = 9/8\nu$ for our $\phi^{(\mathrm{in})}(^{16}\mathrm{O})$ and $\phi^{(\mathrm{in})}(\alpha)$.

We estimate the intrinsic quadrupole moment Q_0 of $\Psi_{LM}(^{20}\mathrm{Ne})$ with $K^\pi = 0^\pm$ by using the simple formula for the quadrupole moment; $Q = -L/(2L+3)\cdot Q_0$.

Table V. Calculated values of the α-spectroscopic factor S_α^2, rms distance $\langle R^2\rangle^{1/2}$ between the c.m. of the ^{16}O and alpha cluster and intrinsic quadrupole moment Q_0 (with no use of effective charge) for the first $K^\pi = 0^\pm$ band states. E_{bound} gives the energy obtained by the bound-state approximation.

(a) HNY-potential case

L^π	E_{bound} (MeV)	S_α^2	$\langle R^2\rangle^{1/2}$ (fm)	Q_0 (e·fm^2)
0^+	−4.86	0.31	3.67	—
2^+	−3.83	0.30	3.64	42.5
4^+	−1.50	0.29	3.55	40.4
6^+	1.97	0.27	3.41	37.1
8^+	6.24	0.25	3.22	33.1
1^-	1.28	0.58	4.49	66.6
3^-	3.09	0.58	4.55	67.3
5^-	6.41	0.57	4.53	66.2
7^-	11.34	0.56	4.43	62.9
9^-	18.05	0.51	4.17	55.6

(b) Volkov-potential case

L^π	E_{bound} (MeV)	S_α^2	$\langle R^2\rangle^{1/2}$ (fm)	Q_0 (e·fm^2)
0^+	−4.26	0.39	4.01	—
2^+	−3.25	0.38	4.00	51.3
4^+	−0.94	0.37	3.90	48.7
6^+	2.52	0.33	3.69	43.6
8^+	6.77	0.27	3.37	36.3
1^-	0.43	0.65	4.68	73.5
3^-	2.17	0.64	4.78	74.2
5^-	5.37	0.64	4.77	73.3
7^-	10.16	0.62	4.69	70.4
9^-	16.80	0.59	4.48	64.2

$S_\alpha^2 = 0.23$ for the $(8, 0)SU_3$ states and $S_\alpha^2 = 0.34$ for fhe $(9, 0)SU_3$ states. The rms radius of the ground state of ^{20}Ne is given by $\langle r^2\rangle_{^{20}\mathrm{Ne}}^{1/2} = 2.87$ fm for the HNY-potential case and $\langle r^2\rangle_{^{20}\mathrm{Ne}}^{1/2} = 2.94$ fm for the Volkov-potential case, while its observed value[28] is 2.90∼2.96 fm. From the observation[39] $Q_0(2_1^+) = 70\pm18$ e·fm^2, while $Q_0(2_1^+) = 52.1$ e·fm^2 in the $(sd)^4$ shell model[12b] with an effective charge 0.5 e; $Q_0 = 29.7$ e·fm^2 for all the $(8, 0)$ SU_3 states ($L>0$) and $Q_0 = 32.8$ e·fm^2 for all the $(9, 0)$ SU_3 states without effective charge.

Calculated values of S_α^2, $\langle R^2\rangle^{1/2}$ and Q_0 are listed in Table V for the states with $L\leq 9$ in the first $K^\pi=0^\pm$ bands. Alpha-correlations grow up more strongly in the lower spin states in each band; in the higher spin states of each band, shrinking of the mass-distribution with increasing spin (or anti-stretching effect)[5),12),18),29)] is seen. For the ground-band state the rms distance $\langle R^2\rangle^{1/2}$ between the ^{16}O and α becomes larger than the value for the $(8,0)SU_3$ state ($\approx$2.9 fm), but still smaller than the sum of the radii of the two clusters ($\approx$4.5 fm). On the other hand, for the first $K^\pi=0^-$ band state the value of $\langle R^2\rangle^{1/2}$ is around the sum of the two radii in the HNY-potential case; this is consistent with the tendency of the reduced α-widths at $a=5$ fm which give about the Wigner limit (see Table IIIa). In the Volkov-potential case, the distance $\langle R^2\rangle^{1/2}$ is somewhat larger than the value in the HNY-potential case for both the $K^\pi=0^\pm$ bands, but it is to be remembered that the reduced α-widths of the Volkov-potential case are considerably too larger than the observed values.

Calculated values of the $B(E2)$ strength for the first $K^\pi=0^\pm$ bands are shown in Table VI (without effective charge). The large deviation from the rotation-model values in the higher spin states is consistent with the above-mentioned anti-stretching effect. It is found in the ground-state band that the calculated $B(E2)$ strengths are still about 60% of the observed strengths provided the observed reduced α-widths of the 6^+ and 8^+ members and the rms radius of the ground state are both reproduced well (in the HNY-potential case; cf. Tables III

Table VI. $B(E2)$ strengths for the ground-state band and the first $K^\pi=0^-$ band in W.u. (here 1 W.u.=3.23 $e^2\cdot fm^4$). Besides the values obtained by the RGM calculation with HNY and Volkov potentials, the values given by the (8, 0) and (9, 0)SU_3 states, by the $(sd)^4$ shell model[12b)] and by the rotational model are listed. The value in the parenthesis is the ratio of the $B(E2)$ strength to that between the lowest two levels in each case.

$K^\pi=0_1^+$	$2^+\rightarrow 0^+$	$4^+\rightarrow 2^+$	$6^+\rightarrow 4^+$	$8^+\rightarrow 6^+$
HNY	11.2 (1.0)	14.0 (1.25)	11.3 (1.01)	6.1 (0.54)
Volkov	16.6 (1.0)	21.0 (1.27)	17.2 (1.04)	9.1 (0.55)
(8, 0) SU_3	5.3 (1.0)	6.7 (1.26)	5.7 (1.07)	3.4 (0.64)
$(sd)^4$	16.3 (1.0)	20.0 (1.23)	16.5 (1.01)	10.2 (0.63)
rotation	— (1.0)	— (1.43)	— (1.57)	— (1.65)
experiment	17.8±2.5 (1.0)	21.9±2.1 (1.23)	20.4±2.4 (1.15)	7.5±2.5 (0.42)
$K^\pi=0_1^-$	$3^-\rightarrow 1^-$	$5^-\rightarrow 3^-$	$7^-\rightarrow 5^-$	$9^-\rightarrow 7^-$
HNY	37.6 (1.0)	41.3 (1.10)	38.0 (1.01)	21.9 (0.74)
Volkov	46.2 (1.0)	51.3 (1.11)	48.7 (1.06)	39.5 (0.86)
(9, 0) SU_3	8.0 (1.0)	8.2 (1.03)	6.6 (0.82)	3.8 (0.48)
rotation	— (1.0)	— (1.18)	— (1.26)	— (1.30)

Only for the $(sd)^4$ shell-model case an effective charge 0.5e is introduced. Experimental values are taken from Ref. 38).

and V). The RGM wave functions adopted here for the ground-band states, however, give the enhanced $B(E2)$ strengths by factor about 2.5 in the HNY-potential case compared with the $(sd)^4$ shell-model calculation[12b] without the effective charge. If we would further include some core-excited configurations*) for the ground-band states beside the closed-shell configuration of the ^{16}O and α in (2·1), then we could expect a certain enhancement in the $B(E2)$ strengths; this new wave function would simultaneously give rise to slight and desirable reduction of the calculated α-widths of the 6^+ and 8^+ members. From the present result we can speculate that for the $(sd)^4$ shell model the effective charge attributed to the inclusion of the excited $(\lambda, 0)SU_3$ states higher than $(8, 0)$ is about 0.32 e, while the charge to be attributed to those core-excited configurations is about 0.14 e.

§ 6. Summary

We have investigated the alpha-clustering structure of ^{20}Ne on the basis of RGM for the $^{16}O+\alpha$ system; use is made of two kinds of nucleon-nucleon potentials, HNY potential of the reaction-matrix type and Volkov potential of the phenomenological type.

The observed level structures, reduced α-widths in the first $K^\pi=0^\pm$ bands and ^{16}O-α threshold energy ($E_x=4.73$ MeV) are simultaneously reproduced well by using HNY potential. The $K^\pi=0^-$ band state has surely the ^{16}O-α molecule-like structure.[2),3)] On the other hand, the ground-band state shows a rather shell-model-like character with a large $(8, 0)SU_3$ component and relatively small excited $(\lambda, 0)$ ones;[7)] however, these excited components of the ground-band states play an important role in the growth of alpha-correlations, for example, in enhancing the α-decay widths of the 6^+ and 8^+ members compared with the shell-model values.[13),14)] The rms distance between the c.m. of the ^{16}O and alpha-cluster is almost the same as the sum of the radii of the two clusters in the first $K^\pi=0^-$ band state ($L\leq 9$), while the distance is much less than the sum in the ground-band state ($L\leq 8$). The alpha cluster is more dissociated in the lower spin states in each of the first $K^\pi=0^\pm$ bands; shrinking of the ^{16}O-α distance is seen in the higher spin states in each band. The calculation with Volkov potential well reproduces the observed level structures of the first $K^\pi=0^\pm$ bands but gives rather too strong alpha-cluster dissociation.

From the behaviour of ^{16}O-α scattering phase shifts (Fig. 3) we can conclude the following. The $K^\pi=0^+$ ground-state band of ^{20}Ne is surely composed of states with spin up to 8, while there appears an excited $K^\pi=0^+$ band with spin up to 12; the resonance states ($L\leq 10$) in the latter band are considered to involve much the $(12, 0)SU_3$ and more-excited $(\lambda, 0)$ configurations in the internal

*) For example, the inclusion of α-^{12}C-α configurations is investigated in Ref. 37) within the framework of the generator coordinate method.

region (cf. Table IV). This excited $K^\pi=0^+$ band is expected to correspond to the observed $K^\pi=0^+$ excited band which starts from the 0^+ level with $E_x\sim 8.6$ MeV and has very large α-widths. The 11^- resonance seems to belong to the first $K^\pi=0^-$ band; this indicates that the state in the band with $L\leq 9$ involves large components of the $(11, 0)SU_3$ and more-excited $(\lambda, 0)$ configurations in the internal region (cf. Table IV).

The role of the exchange kernel has been discussed by showing a kind of effective equivalent-local potential between the ^{16}O and α, and by comparing the result of the RGM calculation with that of the OCM calculation in which the exchange kernel is dropped (cf. Eq. (4·5)). It is found that the kernel gives a repulsive effect in the surface region and an attractive effect in the inner region to the state of the first $K^\pi=0^\pm$ bands (Fig. 4). These effects come mainly from the one-particle exchange and attenuate the probability of finding the alpha cluster in the surface region; especially the ground-band state gets strongly the effects and reduces much the ^{16}O-α molecule-like character from itself. We have given a certain microscopic basis to our phenomenological OCM analysis[9] of α-decay widths in ^{20}Ne; in the analysis the effect of exchange kernel was introduced in a phenomenological way with a parity dependence. It is a subject of the future investigation to explain the effect of the individual part of the two-nucleon potential on the role of exchange kernel and on the alpha-clustering structure of ^{20}Ne taking into account the nuclear saturation property.

Acknowledgements

The authors would like to thank Prof. K. Takada for stimulating discussion and encouragement. We would also like to express our thanks to Prof. R. Tamagaki and Prof. K. Ikeda for encouragement and valuable discussion. We are grateful to Prof. S. Nagata and Dr. Y. Yamamoto for helpful discussion on the two-nucleon potential, especially on HNY potential. Thanks are also due to Prof. A. Arima for stimulating discussion on the structure of ^{20}Ne.

This work was performed as a part of the annual research project on the "Study of Composite Particle Scattering by Microscopic Model" organized by the Research Institute for Fundamental Physics, Kyoto University, Kyoto. We greatly thank Dr. S. Saito, Dr. Y. Abe, Dr. H. Horiuchi and other members of this project for fruitful discussion.

Numerical calculations were carried out on FACOM 230-45 S of the Computation Center of Kyushu University and on FACOM 230-60 of the Computer Center of Kyushu University.

References

1) Prog. Theor. Phys. Suppl. No. 52 (1972), "Alpha-Like Four-Body Correlations and Molecular Aspects in Nuclei".

2) R. H. Davis, *Proceedings of the Third Conference on Reactions between Complex Nuclei, Asilomar, 1963* (University of California Press, Berkeley), p. 67.
3) H. Horiuchi and K. Ikeda, Prog. Theor. Phys. **40** (1968), 277.
4) J. Hiura, Y. Abe, S. Saito and O. Endo, Prog. Theor. Phys. **42** (1969), 555.
5) H. Horiuchi, Soryusiron Kenkyu (mimeographed circular in Japanese) **39** (1969), 260; **41** (1970), D26.
6) F. Nemoto and H. Bando, Prog. Theor. Phys. **47** (1972), 1210.
7) M. Kamimura, T. Matsuse and K. Takada, Prog. Theor. Phys. **47** (1972), 1537.
8) W. Sünkel and K. Wildermuth, Phys. Letters **41B** (1972), 439.
9) T. Matsuse and M. Kamimura, Prog. Theor. Phys. **49** (1973), 1765.
10) H. Horiuchi and Y. Suzuki, Prog. Theor. Phys. **49** (1973), 1974.
11) F. Tanabe and F. Nemoto, Prog. Theor. Phys. **51** (1974), 2009.
12a) Y. Akiyama, A. Arima and T. Sebe, Nucl. Phys. **A138** (1969), 273.
b) A. Arima, M. Sakakura and T. Sebe, Nucl. Phys. **A170** (1971), 273.
13a) A. Arima and S. Yoshida, Phys. Letters **40B** (1972), 15.
b) A. Arima and S. Yoshida, Nucl. Phys. **A219** (1974), 475.
14) K. Yazaki, Prog. Theor. Phys. **49** (1973), 1205.
15) S. Saito, Prog. Theor. Phys. **41** (1969), 705.
16) J. A. Wheeler, Phys. Rev. **52** (1937), 1083, 1107.
K. Wildermuth and W. McClure, "Cluster Representation of Nuclei", Springer Tracts in Modern Physics Vol. **41** (1966), 1.
17) A. Hasegawa and S. Nagata, Prog. Theor. Phys. **45** (1971), 1786.
18a) Y. Yamamoto, Prog. Theor. Phys. **52** (1974), 471.
b) S. Nagata and Y. Yamamoto, private communication.
19) A. B. Volkov, Nucl. Phys. **74** (1965), 33.
20) M. Kamimura and T. Matsuse, Prog. Theor. Phys. **51** (1974), 438.
21) Y. Suzuki, Prog. Theor. Phys. **50** (1972), 341.
22) R. Tamagaki, Prog. Theor. Phys. **39** (1968), 91.
23) R. Tamagaki, Prog. Theor. Phys. Suppl. Extra Number (1968), 242.
24) H. Bando, S. Nagata and Y. Yamamoto, Prog. Theor. Phys. **44** (1970), 646.
25a) P. Heiss and H. H. Hackenbroich, Z. Phys. **235** (1970), 422.
b) M. Kamimura, Soryusiron Kenkyu (mimeographed circular in Japanese) **50** (1974), C27.
26) W. Kohn, Phys. Rev. **74** (1948), 1763.
27) A. M. Lane, Rev. Mod. Phys. **32** (1960), 519.
28) Y. Horikawa, Prog. Theor. Phys. **47** (1972), 867.
Y. Horikawa, A. Nakada and Y. Torizuka, Prog. Theor. Phys. **49** (1973), 2005.
29) H. C. Lee and R. Y. Cusson, Phys. Rev. Letters **29** (1972), 1525.
30) D. M. Brink and E. Boeker, Nucl. Phys. **A91** (1967), 1.
31) T. Ando, K. Ikeda and Y. Suzuki, private communication.
32) S. Ohkubo, H. Horiuchi, Y. Suzuki and A. Tohsaki, private communication.
33) A. Arima and T. Tomoda, private communication.
34) B. F. Bayman and A. Bohr, Nucl. Phys. **2** (1958/59), 596.
35) A. Arima, V. Gillet and J. Ginocchio, Phys. Rev. Letters **25** (1970), 1043.
36) D. Strottman, N. Anyas-Weiss, J. C. Cornell, P. S. Fisher, P. N. Hudson, A. Menchaca-Rocha, A. D. Panagiotou and D. K. Scott, Phys. Letters **47B** (1973), 16.
37) H. Horiuchi, K. Ikeda, F. Nemoto, Y. Suzuki and Y. Yamamoto, private communication.
38) F. Ajzenberg-Selove, Nucl. Phys. **A166** (1972), 1.
39) D. K. Olsen, A. R. Barnett, S. F. Biagi, N. H. Merrill and W. R. Phillips, Nucl. Phys. **A220** (1974), 541.